

# Magnetic dipole moment of the $\Delta^+(1232)$ from the $\gamma p \rightarrow \gamma \pi^0 p$ reaction

D. Drechsel and M. Vanderhaeghen

*Institut für Kernphysik, Johannes-Gutenberg-Universität, D-55099 Mainz, Germany*

(November 5, 2018)

## Abstract

The  $\gamma p \rightarrow \gamma \pi^0 p$  reaction in the  $\Delta(1232)$ -resonance region is investigated as a method to access the  $\Delta^+(1232)$  magnetic dipole moment. The calculations are performed within the context of an effective Lagrangian model containing both the  $\Delta$ -resonant mechanism and a background of non-resonant contributions to the  $\gamma p \rightarrow \gamma \pi^0 p$  reaction. Results are shown both for existing and forthcoming  $\gamma p \rightarrow \gamma \pi^0 p$  experiments. In particular, the sensitivity of unpolarized cross sections and photon asymmetries to the  $\Delta^+$  magnetic dipole moment is displayed for those forthcoming data.

PACS numbers : 12.39.Jh, 13.60.Fz, 14.20.Gk

arXiv:hep-ph/0105060v1 7 May 2001

## I. INTRODUCTION

The static properties of baryons constitute an important test for theoretical descriptions in the non-perturbative domain of QCD. In particular, different predictions for the magnetic moments of baryons were made in quark-models, chiral quark soliton models, and lattice QCD calculations (see e.g. Ref. [1]).

The experimental values for the magnetic moments of octet baryons ( $N, \Lambda, \Sigma, \Xi$ ) are known accurately through spin precession measurements. For decuplet baryons, only the magnetic moment of the  $\Omega^-$  could be determined through such techniques, because the other decuplet baryons have too short lifetimes.

In particular the magnetic dipole moment of the  $\Delta(1232)$  resonance is of considerable theoretical interest. If SU(6) symmetry holds, then the nucleon and the  $\Delta$  resonance are degenerate and their magnetic moments are related through  $\mu_\Delta = e_\Delta \mu_p$ , where  $e_\Delta$  is the  $\Delta$  electric charge, and  $\mu_p$  the proton magnetic moment. However, different theoretical models predict considerable deviations from this SU(6) value [2].

In the past, it has been proposed to determine the magnetic moment of the  $\Delta^{++}(1232)$  by measuring the  $\pi^+p \rightarrow \gamma\pi^+p$  reaction [3], and the first dedicated experiment of this type has been performed in the '70s [4]. As a result of these measurements [4,5], and using different theoretical analyses, the PDG [6] quotes the range :  $\mu_{\Delta^{++}} = 3.7 - 7.5 \mu_N$  (where  $\mu_N$  is the nuclear magneton), while SU(6) symmetry results in the value  $\mu_{\Delta^{++}} = 5.58 \mu_N$ . The large uncertainty in the extraction of  $\mu_{\Delta^{++}}$  from the data is due to large non-resonant contributions to the  $\pi^+p \rightarrow \gamma\pi^+p$  reaction because of bremsstrahlung from the charged pion ( $\pi^+$ ) and proton (p).

As an alternative method, it has been proposed [7] to determine the magnetic moment of the  $\Delta^+(1232)$  through measurement of the  $\gamma p \rightarrow \gamma\pi^0 p$  reaction. First calculations for this reaction, including only the resonant mechanism, have been recently performed in Refs. [8,9]. Due to the small cross sections for this reaction, which is proportional to  $\alpha_{em}^2 = 1/(137)^2$ , a first measurement has only now been performed by the A2/TAPS collaboration at MAMI [10]. In the near future, such experiments can be performed with much higher count rates by using  $4\pi$  detectors, such as planned e.g. by using the Crystal Ball detector at MAMI [11].

It is the aim of the present work to perform detailed calculations of the  $\gamma p \rightarrow \gamma' \pi^0 p$  reaction, which include both resonant and non-resonant mechanisms, and to investigate in detail the sensitivity of this reaction to the  $\Delta^+(1232)$  magnetic dipole moment.

In Sec. II, we start by specifying the kinematics and cross section of the  $\gamma p \rightarrow \gamma\pi^0 p$  reaction.

In Sec. III, we describe in detail the effective Lagrangian model for the  $\gamma p \rightarrow \gamma\pi^0 p$  reaction in the  $\Delta(1232)$  resonance region. Besides resonant mechanisms which contain the  $\Delta^+$  magnetic moment contribution, the model also includes the main non-resonant contributions to this reaction. It is shown how the model for the  $\gamma p \rightarrow \gamma\pi^0 p$  process is obtained from an analogous model for the  $\gamma p \rightarrow \pi^0 p$  process by coupling a photon in a gauge invariant way to this latter process. Special attention is paid to the constraint which gauge invariance imposes on the electromagnetic coupling of a photon to a resonance of finite width, which has been discussed extensively in the literature in recent years for the analogous case of the  $W^\pm$  gauge boson for which very accurate data have become available.

We then show in Sec. IV, within the context of the developed effective Lagrangian model, the results for the  $\gamma p \rightarrow \gamma \pi^0 p$  reaction, for both existing and forthcoming experiments. In particular, we study the sensitivity of both unpolarized cross sections and photon asymmetries to the  $\Delta^+$  magnetic dipole moment.

Finally, we present our conclusions and an outlook in Sec. V.

## II. KINEMATICS AND CROSS SECTION FOR THE $\gamma P \rightarrow \gamma \pi^0 P$ REACTION

In the  $\gamma p \rightarrow \gamma \pi^0 p$  process, a photon (with four-momentum  $k$  and helicity  $\lambda$ ) scatters on a proton target (with four-momentum  $p_N$ , and spin projection  $s_N$ ), and a photon (with four-momentum  $k'$  and helicity  $\lambda'$ ), a  $\pi^0$  (with four-momentum  $p_\pi$ ) and a proton (with four-momentum  $p'_N$ , spin projection  $s'_N$ ) can be observed in the final state.

The kinematics of the  $\gamma p \rightarrow \gamma \pi^0 p$  reaction is characterized by 5 variables. First, the total c.m. energy squared is given by the usual Mandelstam invariant  $s = (k + p_N)^2$ . Equivalently to  $s$ , we will use the energy of the initial photon  $E_\gamma^{c.m.}$  in the c.m. system of the initial  $\gamma p$  system (total c.m. system). Furthermore, there are two variables which characterize the photon in the total c.m. system : its energy  $E'_\gamma^{c.m.}$  and polar angle  $\Theta_\gamma^{c.m.}$  respectively. Finally, two more variables are needed to specify the kinematics of the 3-body final state completely. For convenience, we choose them to be the pion angles in the rest frame of the  $\pi^0 p$  system w.r.t. the direction of the c.m. momentum vector of the  $\pi^0 p$  system :  $\Theta_\pi^*$  denotes the polar angle of the pion, and  $\Phi_\pi^*$  is its azimuthal angle. From these variables, one can reconstruct the invariant mass of the  $\pi^0 p$  system as :

$$W_{\pi^0 p}^2 = s - 2\sqrt{s} E_\gamma^{c.m.}, \quad (1)$$

and the pion momentum in the  $\pi^0 p$  rest frame is calculated as :

$$|\vec{p}_\pi^*|^2 = \frac{1}{4W_{\pi^0 p}^2} \left\{ W_{\pi^0 p}^4 - 2W_{\pi^0 p}^2 (m_\pi^2 + M_N^2) + (M_N^2 - m_\pi^2)^2 \right\}. \quad (2)$$

The unpolarized cross section for the  $\gamma p \rightarrow \gamma \pi^0 p$  reaction, which is differential w.r.t. the outgoing photon energy and angles in the c.m. system, and differential w.r.t. the pion angles in the  $\pi^0 p$  rest frame is given by :

$$\begin{aligned} \frac{d\sigma}{dE_\gamma^{c.m.} d\Omega_\gamma^{c.m.} d\Omega_\pi^*} &= \frac{1}{(2\pi)^5} \frac{1}{32\sqrt{s}} \frac{E_\gamma^{c.m.}}{E_\gamma^{c.m.}} \frac{|\vec{p}_\pi^*|}{W_{\pi^0 p}} \\ &\times \left( \frac{1}{4} \sum_\lambda \sum_{s_N} \sum_{\lambda'} \sum_{s'_N} |\varepsilon_\mu(k, \lambda) \varepsilon_\nu^*(k', \lambda') \mathcal{M}^{\nu\mu}|^2 \right), \quad (3) \end{aligned}$$

where  $\varepsilon_\mu(k, \lambda)$  ( $\varepsilon_\nu^*(k', \lambda')$ ) are the polarization vectors of the incoming (outgoing) photons respectively. In Eq. (3),  $\mathcal{M}^{\nu\mu}$  is the tensor for the  $\gamma p \rightarrow \gamma \pi^0 p$  process which will be calculated in Sec. III within the context of an effective Lagrangian model.

Further on, we will show results for partially integrated cross sections of the  $\gamma p \rightarrow \gamma \pi^0 p$  reaction, e.g. the cross section  $d\sigma/dE_\gamma^{c.m.}$  differential w.r.t. the outgoing photon c.m. energy, or the cross section  $d\sigma/d\Omega_\gamma^{c.m.}$  differential w.r.t. the photon c.m. solid angle. Those are obtained by integrating the fully differential cross section of Eq. (3) over the appropriate variables.

### III. EFFECTIVE LAGRANGIAN MODEL FOR THE $\gamma P \rightarrow \gamma \pi^0 P$ REACTION IN THE $\Delta(1232)$ RESONANCE REGION

#### A. $\Delta(1232)$ resonance processes

In order to calculate the resonant  $\Delta(1232)$  contribution to the  $\gamma p \rightarrow \gamma \pi^0 p$  reaction, we start from the  $\Delta(1232)$ -resonance contribution to the  $\gamma p \rightarrow \pi^0 p$  process, corresponding to Fig. 1(a).

We describe the  $\Delta$ -resonance in the Rarita-Schwinger formalism. It is well known that the description of a spin-3/2 field, such as the  $\Delta$ -resonance, through a Rarita-Schwinger field, introduces an arbitrary parameter (usually called  $A$  in the literature, see e.g. [14]). This parameter arises when removing the spin-1/2 component of the vector-spinor Rarita-Schwinger field, through a contact transformation. Physical quantities, describing a spin-3/2 particle, should however be independent of this parameter  $A$  and therefore care has to be taken in the calculations that the  $A$ -dependence of the  $\Delta$  vertices ( $\gamma N \Delta$ ,  $\pi N \Delta$ ) and  $\Delta$  propagator cancel. We follow here the procedure of Refs. [12,13], where it was shown that the  $A$ -dependent Feynman rules involving the  $\Delta$  can be replaced by a set of  $A$ -independent ‘reduced’ vertices and propagator. In this framework, the reduced  $\Delta$ -propagator  $\tilde{G}_{\alpha\beta}(p_\Delta)$  is given by [12] :

$$\begin{aligned} \tilde{G}_{\alpha\beta}(p_\Delta) = & \frac{\not{p}_\Delta + M_\Delta}{p_\Delta^2 - M_\Delta^2} \left\{ -g_{\alpha\beta} + \frac{1}{3} \gamma_\alpha \gamma_\beta + \frac{1}{3M_\Delta} (\gamma_\alpha (p_\Delta)_\beta - \gamma_\beta (p_\Delta)_\alpha) + \frac{2}{3M_\Delta^2} (p_\Delta)_\alpha (p_\Delta)_\beta \right\} \\ & - \frac{2}{3M_\Delta^2} \left\{ \gamma_\alpha (p_\Delta)_\beta + \gamma_\beta (p_\Delta)_\alpha - \gamma_\alpha (\not{p}_\Delta - M_\Delta) \gamma_\beta \right\}, \end{aligned} \quad (4)$$

where  $\alpha$  and  $\beta$  are the  $\Delta$  four-vector indices,  $p_\Delta$  is the four-momentum and  $M_\Delta$  the mass of the  $\Delta$ . To take account of the finite width of the  $\Delta$ -resonance, we follow the procedure of [12,13] by using a complex pole description for the  $\Delta$ -resonance excitation. This amounts to the replacement :

$$M_\Delta \rightarrow M_\Delta - \frac{i}{2} \Gamma_\Delta, \quad (5)$$

in the propagator of Eq. (4). For the complex pole parameter of the  $\Delta(1232)$ -resonance, we use the values given by the PDG [6] :  $M_\Delta = 1210$  MeV,  $\Gamma_\Delta = 100$  MeV. Further on, when calculating the  $\Delta$ -resonance contribution to the  $\gamma p \rightarrow \gamma \pi^0 p$  process, we will discuss that this ‘complex mass scheme’ guarantees electromagnetic gauge invariance, in contrast to using Breit-Wigner propagators with energy-dependent widths.

With the propagator of Eq. (4), the amplitude for the  $\Delta(1232)$ -resonance contribution to the  $\gamma p \rightarrow \pi^0 p$  process, corresponding to Fig. 1(a), is then given by :

$$\begin{aligned} \varepsilon_\mu(k, \lambda) \mathcal{M}_a^\mu(\gamma p \rightarrow \pi^0 p) = & i e \frac{2}{3} \frac{f_{\pi N \Delta}}{m_\pi} (p_\pi)^\alpha \varepsilon_\mu(k, \lambda) \\ & \times \bar{N}(p'_N, s'_N) \tilde{G}_{\alpha\beta}(p_\Delta) \left[ G_M \Gamma_M^{\beta\mu} + G_E \Gamma_E^{\beta\mu} \right] N(p_N, s_N), \end{aligned} \quad (6)$$

where  $\varepsilon_\mu$  is the photon four-vector,  $e$  is the proton electric charge ( $\alpha_{em} = e^2/(4\pi) = 1/137$ ) and  $m_\pi$  the pion mass. The  $\pi N \Delta$  coupling constant  $f_{\pi N \Delta}$  in Eq. (6) is taken from the

$\Delta \rightarrow \pi N$  decay, which yields :  $f_{\pi N \Delta} \approx 1.95$ . Furthermore, in Eq. (6),  $\Gamma_M^{\beta\mu}$  ( $\Gamma_E^{\beta\mu}$ ) denote the magnetic (electric)  $\gamma N \Delta$  vertices respectively, and are defined as :

$$\Gamma_M^{\beta\mu} = -\frac{3}{2M_N} \frac{1}{(M_N + M_\Delta)} \varepsilon^{\beta\mu\kappa\lambda} \frac{1}{2} (p_\Delta + p_N)_\kappa k_\lambda \quad (7)$$

$$\begin{aligned} \Gamma_E^{\beta\mu} &= -\Gamma_M^{\beta\mu} - \frac{6}{(M_\Delta + M_N)(M_\Delta - M_N)^2 M_N} \\ &\times \left( \varepsilon^{\beta\sigma\kappa\lambda} \frac{1}{2} (p_\Delta + p_N)_\kappa k_\lambda \right) \left( \varepsilon^\mu{}_\sigma{}^{\rho\tau} (p_\Delta)_\rho k_\tau \right) i \gamma_5. \end{aligned} \quad (8)$$

The magnetic  $\gamma N \Delta$  coupling  $G_M$  at the real photon point is taken from the MAID00 analysis :  $G_M(0) = 3.02$  [15]. The small electric  $\gamma N \Delta$  coupling  $G_E$ , corresponding to the  $E2/M1$  ratio of about -2.5% for the  $\gamma N \rightarrow \Delta(1232)$  transition [16], can be safely neglected for the sake of our subsequent analysis.

Starting from the  $\Delta$ -contribution of Eq. (6) to the  $\gamma p \rightarrow \pi^0 p$  process, we now construct the corresponding  $\Delta$ -contribution to the  $\gamma p \rightarrow \gamma \pi^0 p$  process. This is obtained by coupling a photon in a gauge invariant way to all charged particles in Fig. 1(a). This way we obtain in the first place the diagrams with a photon attached to an external proton (Figs. 2(a1) and (a3)). Their contributions to the tensor  $\mathcal{M}^{\nu\mu}$  of Eq. (3) is given by :

$$\begin{aligned} \mathcal{M}_{a1}^{\nu\mu}(\gamma p \rightarrow \gamma \pi^0 p) &= i e^2 \frac{2}{3} \frac{f_{\pi N \Delta}}{m_\pi} (p_\pi)^\alpha \\ &\times \bar{N}(p'_N, s'_N) \tilde{G}_{\alpha\beta}(p'_\Delta) \left[ G_M \Gamma_M^{\beta\mu} + G_E \Gamma_E^{\beta\mu} \right] \\ &\times \frac{(\not{p}'_N - \not{k}' + M_N)}{-2 p_N \cdot k'} \left[ \gamma^\nu - \kappa_p i \sigma^{\nu\rho} \frac{k'_\rho}{2M_N} \right] N(p_N, s_N), \end{aligned} \quad (9)$$

$$\begin{aligned} \mathcal{M}_{a3}^{\nu\mu}(\gamma p \rightarrow \gamma \pi^0 p) &= i e^2 \frac{2}{3} \frac{f_{\pi N \Delta}}{m_\pi} (p_\pi)^\alpha \\ &\times \bar{N}(p'_N, s'_N) \left[ \gamma^\nu - \kappa_p i \sigma^{\nu\rho} \frac{k'_\rho}{2M_N} \right] \frac{(\not{p}'_N + \not{k}' + M_N)}{2 p'_N \cdot k'} \tilde{G}_{\alpha\beta}(p_\Delta) \\ &\times \left[ G_M \Gamma_M^{\beta\mu} + G_E \Gamma_E^{\beta\mu} \right] N(p_N, s_N), \end{aligned} \quad (10)$$

where we also included, besides the electric coupling of the emitted photon to the proton, the magnetic contribution ( $\kappa_p = 1.79$  is the proton anomalous magnetic moment). In the soft-photon limit ( $k' \rightarrow 0$ ), the coupling of the photon to the external lines gives the only contribution. However, at finite energy for the emitted photon, gauge invariance also requires the diagram with a photon attached to the intermediate  $\Delta^+$  (Fig.2(a2)), which corresponds to the tensor :

$$\begin{aligned} \mathcal{M}_{a2}^{\nu\mu}(\gamma p \rightarrow \gamma \pi^0 p) &= -i e^2 \frac{2}{3} \frac{f_{\pi N \Delta}}{m_\pi} (p_\pi)^\alpha \\ &\times \bar{N}(p'_N, s'_N) \tilde{G}_{\alpha\beta}(p'_\Delta) \Gamma_{\gamma\Delta\Delta}^{\nu\beta\beta'} \tilde{G}_{\beta'\delta}(p_\Delta) \left[ G_M \Gamma_M^{\delta\mu} + G_E \Gamma_E^{\delta\mu} \right] N(p_N, s_N), \end{aligned} \quad (11)$$

where  $\Gamma_{\gamma\Delta\Delta}$  is the  $\gamma\Delta\Delta$  vertex :

$$\Gamma_{\gamma\Delta\Delta}^{\nu\beta\beta'} = g^{\beta\beta'} \left( \gamma^\nu - i \kappa_\Delta \sigma^{\nu\lambda} \frac{k'_\lambda}{2M_\Delta} \right) + \frac{1}{3} \left( \gamma^\beta \gamma^\nu \gamma^{\beta'} - \gamma^\beta g^{\nu\beta'} - \gamma^{\beta'} g^{\nu\beta} \right), \quad (12)$$

containing the photon coupling to a spin 3/2 field of a point-like particle (i.e.  $\kappa_\Delta = 0$ ) [12], as well as the  $\Delta$  anomalous magnetic dipole moment contribution, which is proportional to  $\kappa_\Delta$ .

The vertex for a point- spin-3/2 particle follows from the requirement of gauge invariance. Indeed, only the sum of the 3 diagrams Fig. 2(a1,a2,a3) is gauge-invariant, which is expressed through the electromagnetic Ward identity relating the  $\gamma\Delta\Delta$  vertex and the  $\Delta$ -reduced propagator :

$$\left(p'_\Delta - p_\Delta\right)_\nu \tilde{G}_{\alpha\kappa}(p'_\Delta) \Gamma_{\gamma\Delta\Delta}^{\nu\kappa\lambda} \tilde{G}_{\lambda\beta}(p_\Delta) = -\tilde{G}_{\alpha\beta}(p_\Delta) + \tilde{G}_{\alpha\beta}(p'_\Delta). \quad (13)$$

To include the finite width of the  $\Delta$ , the ‘complex mass scheme’ was advocated in Ref. [12], i.e. the replacement of  $M_\Delta$  by the complex mass of Eq. (5) *everywhere* in the propagator Eq. (4), and not only in its denominator. In doing so, it is easily checked that the Ward identity of Eq. (13) still holds. On the other hand, when using Breit-Wigner propagators, replacing  $M_\Delta^2$  in the denominator of Eq. (4) by  $M_\Delta^2 - i M_\Delta \Gamma_\Delta(W)$ , and with  $\Gamma_\Delta(W)$  an energy dependent width, the  $\Delta$  propagators before and after the emission of the photon have different widths (except in the soft-photon limit  $k' \rightarrow 0$ , where the contribution of diagram Fig. 2(a2) vanishes relative to those of Fig. 2(a1) and (a3)). Therefore, when using energy-dependent widths at finite energy of the emitted photon, it is not possible to maintain the Ward identity of Eq. (13) with the point vertex ( $\kappa_\Delta = 0$ ) of Eq. (12).

In recent years, the issue of a gauge invariant definition of resonant masses, widths and partial widths has newly received attention in view of high precision measurements of the properties of the  $W$  and  $Z$  gauge bosons at LEP [17–20]. In particular, it has been shown in Refs. [17–20] that a complex pole definition of a resonance provides a systematic way to maintain gauge invariance of the amplitude at any order of perturbation theory. In particular, one-loop corrections to  $W^\pm$  propagators and vertices have been calculated through a fermion loop [21,22], and it has been shown in the limit of massless fermions (leptons, quarks) in the loop that the simplest prescription to obtain gauge invariant amplitudes in the presence of finite width effects is to perform a Laurent expansion of the full amplitude around the complex pole position of the resonance [20]. A similar observation has been made in Ref. [23], where the  $\rho^\pm$  vector meson contribution to the  $\tau \rightarrow \pi\pi\nu\gamma$  decay has been studied as a source to extract the magnetic dipole moment of the  $\rho$  meson. The absorptive one-loop corrections to the propagator and vertices of the charged  $\rho$  vector meson were calculated in Ref. [23] through a pion loop. In the limit of vanishing mass of the pions in the loop, it was further shown that the ‘complex mass scheme’, replacing the  $\rho$  mass by a complex parameter in the lowest order expressions for propagators and vertices, provides a gauge invariant description in the presence of the finite width of the  $\rho$  meson.

This ‘complex mass scheme’ prescription was then applied in Ref. [13] to the propagator and vertices of the  $\Delta^{++}$  resonance, in the description of the  $\pi^+p \rightarrow \gamma\pi^+p$  reaction. It was argued for the  $\Delta$  resonance, similar to the spin-1 case, that the constraint imposed by gauge invariance leads to this complex mass scheme. An explicit calculation of the absorption corrections to  $\Delta$  propagator and vertices through  $\pi N$  loops would be very valuable to check this conjecture. In this work, we will follow the ‘complex mass scheme’ prescription of Eq. (5), and apply it to the description of the  $\Delta^+$  resonance in the  $\gamma p \rightarrow \gamma\pi^0 p$  process. This guarantees electromagnetic gauge invariance as expressed in Eq. (13).

Besides the vertex for a point particle of spin 3/2, which is constrained by gauge invariance,

we also included in Eq. (12) the contribution of the  $\Delta$  anomalous magnetic dipole moment, proportional to  $\kappa_\Delta$ . This magnetic moment contribution is gauge invariant by itself. The extraction of the value of  $\kappa_\Delta$  is the principal motivation for constructing the present model to analyse the  $\gamma p \rightarrow \gamma \pi^0 p$  reaction. The  $\Delta^+$  magnetic moment  $\mu_{\Delta^+}$  is then obtained from the  $\Delta^+$  anomalous magnetic moment  $\kappa_{\Delta^+}$  as :

$$\mu_{\Delta^+} \equiv (1 + \kappa_{\Delta^+}) \frac{e}{2M_\Delta} = (1 + \kappa_{\Delta^+}) \frac{M_N}{M_\Delta} \mu_N, \quad (14)$$

where  $\mu_N \equiv e/(2M_N)$  is the usual nuclear magneton. The SU(6) value predicts the value  $\kappa_{\Delta^+} = \kappa_p = 1.79$ . Assuming SU(2) isospin symmetry, the PDG range for  $\mu_{\Delta^{++}}$  corresponds for  $\Delta^+$  to the range  $\mu_{\Delta^+} = 1.85 - 3.75 \mu_N$ , which translates to the range  $\kappa_{\Delta^+} = 1.43 - 3.92$ .

In addition to the magnetic dipole moment (M1), the  $\Delta(1232)$  also has static monopole and quadrupole Coulomb moments (C0, C2) and a magnetic octupole moment (M3). It is obvious that the Coulomb moment does not couple to the emitted photon, and the magnetic octupole moment is suppressed by two additional powers in the photon momentum. There is, in principle, a contribution from electric (transverse) quadrupole radiation (E2). However this is strongly suppressed by the fact that E2 radiation vanishes by time-reversal invariance if the initial and final states are exactly the same. In fact, such radiation can only contribute by off-shell and recoil effects of the intermediate resonance. In view of the small ratio  $R = E2/M1 \approx -2.5\%$  for the  $N\Delta$  transition, it is therefore (unfortunately !) very unlikely that one will ever learn about the quadrupole moment of the  $\Delta(1232)$  by radiative pion photoproduction. In the present description, we therefore keep only the magnetic dipole moment of the  $\Delta(1232)$ .

## B. Vector meson ( $\omega$ ) exchange processes

Although the  $\gamma p \rightarrow \pi^0 p$  process in the  $\Delta(1232)$  resonance region is dominated by the  $\Delta$ -excitation process, it is well known that an accurate description also necessitates the inclusion of non-resonant mechanisms. In the following, we discuss such non-resonant mechanisms and calculate them for the  $\gamma p \rightarrow \gamma \pi^0 p$  process.

At the high energy side of the  $\Delta(1232)$ -region, the prominent non-resonant contribution to the  $\gamma p \rightarrow \pi^0 p$  reaction comes from vector-meson exchange, dominantly  $\omega$ -exchange as shown in Fig. 1(b). The amplitude of the  $\omega$ -exchange contribution is given by :

$$\begin{aligned} \varepsilon_\mu(k, \lambda) \mathcal{M}_b^\mu(\gamma p \rightarrow \pi^0 p) &= -ie g_{\omega NN} \frac{g_{\omega\pi\gamma}}{m_\pi} \frac{1}{t - m_\omega^2} \varepsilon^{\lambda\mu\alpha\beta} k_\lambda (k - p_\pi)_\alpha \varepsilon_\mu(k, \lambda) \\ &\times \bar{N}(p'_N, s'_N) \left[ \gamma_\beta + \kappa_\omega i\sigma_{\beta\sigma} \frac{(k - p_\pi)^\sigma}{2M_N} \right] N(p_N, s_N), \end{aligned} \quad (15)$$

where  $m_\omega = 0.7826$  GeV is the  $\omega$ -meson mass. The  $\omega\pi\gamma$  coupling  $g_{\omega\pi\gamma}$  is well known from the radiative decay  $\omega \rightarrow \pi\gamma$ , which leads to the value :  $g_{\omega\pi\gamma} = 0.314$ . The  $\omega NN$  coupling  $g_{\omega NN}$  is taken from a high-energy analysis of  $\gamma p \rightarrow \pi^0 p$  :  $g_{\omega NN} = 15$  [24]. The (isoscalar) tensor coupling  $\kappa_\omega$  is generally found to be small and is set equal to zero in the present analysis, i.e.  $\kappa_\omega = 0$ .

When coupling a photon in a gaugeinvariant way to both charged proton lines in Fig. 1(b),

one obtains the corresponding diagrams of Fig. 2(b1) and (b2) for the  $\gamma p \rightarrow \gamma \pi^0 p$  reaction. Their contributions to the tensor  $\mathcal{M}^{\nu\mu}$  of Eq. (3) are given by :

$$\begin{aligned} \mathcal{M}_{b1}^{\nu\mu}(\gamma p \rightarrow \gamma \pi^0 p) &= -ie^2 g_{\omega NN} \frac{g_{\omega\pi\gamma}}{m_\pi} \frac{1}{t - m_\omega^2} \varepsilon^{\lambda\mu\alpha\beta} k_\lambda (k - p_\pi)_\alpha \\ &\times \bar{N}(p'_N, s'_N) \left[ \gamma_\beta + \kappa_\omega i\sigma_{\beta\sigma} \frac{(k - p_\pi)^\sigma}{2M_N} \right] \\ &\times \frac{(\not{p}'_N - \not{k}' + M_N)}{-2p_N \cdot k'} \left[ \gamma^\nu - \kappa_p i\sigma^{\nu\rho} \frac{k'_\rho}{2M_N} \right] N(p_N, s_N), \end{aligned} \quad (16)$$

$$\begin{aligned} \mathcal{M}_{b2}^{\nu\mu}(\gamma p \rightarrow \gamma \pi^0 p) &= -ie^2 g_{\omega NN} \frac{g_{\omega\pi\gamma}}{m_\pi} \frac{1}{t - m_\omega^2} \varepsilon^{\lambda\mu\alpha\beta} k_\lambda (k - p_\pi)_\alpha \\ &\times \bar{N}(p'_N, s'_N) \left[ \gamma^\nu - \kappa_p i\sigma^{\nu\rho} \frac{k'_\rho}{2M_N} \right] \frac{(\not{p}'_N + \not{k}' + M_N)}{2p'_N \cdot k'} \\ &\times \left[ \gamma_\beta + \kappa_\omega i\sigma_{\beta\sigma} \frac{(k - p_\pi)^\sigma}{2M_N} \right] N(p_N, s_N), \end{aligned} \quad (17)$$

### C. Born term contributions

At the low energy side of the  $\Delta(1232)$ -region, the prominent non-resonant contribution to the  $\gamma p \rightarrow \pi^0 p$  reaction comes from the Born contributions as shown in Fig. 1(c1) and (c2). They are evaluated here using pseudo-vector  $\pi NN$  coupling, which yields the amplitudes :

$$\begin{aligned} \varepsilon_\mu(k, \lambda) \mathcal{M}_{c1}^\mu(\gamma p \rightarrow \pi^0 p) &= -e \frac{f_{\pi NN}}{m_\pi} \varepsilon_\mu(k, \lambda) \bar{N}(p'_N, s'_N) \not{p}'_N \gamma_5 \frac{(\not{p}'_N + \not{k} + M_N)}{2p_N \cdot k} \\ &\times \left[ \gamma^\mu + \kappa_p i\sigma^{\mu\rho} \frac{k_\rho}{2M_N} \right] N(p_N, s_N), \end{aligned} \quad (18)$$

$$\begin{aligned} \varepsilon_\mu(k, \lambda) \mathcal{M}_{c2}^\mu(\gamma p \rightarrow \pi^0 p) &= -e \frac{f_{\pi NN}}{m_\pi} \varepsilon_\mu(k, \lambda) \bar{N}(p'_N, s'_N) \left[ \gamma^\mu + \kappa_p i\sigma^{\mu\rho} \frac{k_\rho}{2M_N} \right] \\ &\times \frac{(\not{p}'_N - \not{k} + M_N)}{-2p'_N \cdot k} \not{p}'_N \gamma_5 N(p_N, s_N). \end{aligned} \quad (19)$$

The  $\pi NN$  coupling constant is given by its well known value :  $f_{\pi NN}^2/(4\pi) = 0.08$  [25].

The corresponding contributions to the  $\gamma p \rightarrow \gamma \pi^0 p$  reaction are obtained by coupling a photon in a gauge invariant way to all proton lines in Fig. 1(c1) and (c2). This yields the six diagrams of Fig. 2(c1-c6) whose contributions to the tensor  $\mathcal{M}^{\nu\mu}$  of Eq. (3) are given by :

$$\begin{aligned} \mathcal{M}_{c1}^{\nu\mu}(\gamma p \rightarrow \gamma \pi^0 p) &= -e^2 \frac{f_{\pi NN}}{m_\pi} \bar{N}(p'_N, s'_N) \not{p}'_N \gamma_5 \frac{(\not{p}'_N + \not{k} - \not{k}' + M_N)}{2p_N \cdot (k - k') - 2k \cdot k'} \\ &\times \left[ \gamma^\mu + \kappa_p i\sigma^{\mu\rho} \frac{k_\rho}{2M_N} \right] \frac{(\not{p}'_N - \not{k}' + M_N)}{-2p_N \cdot k'} \left[ \gamma^\nu - \kappa_p i\sigma^{\nu\sigma} \frac{k'_\sigma}{2M_N} \right] N(p_N, s_N), \end{aligned} \quad (20)$$

$$\mathcal{M}_{c2}^{\nu\mu}(\gamma p \rightarrow \gamma \pi^0 p) = -e^2 \frac{f_{\pi NN}}{m_\pi} \bar{N}(p'_N, s'_N) \not{p}'_N \gamma_5 \frac{(\not{p}'_N + \not{k} - \not{k}' + M_N)}{2p_N \cdot (k - k') - 2k \cdot k'}$$



$$\times \left[ \gamma^\nu - \kappa_p i\sigma^{\nu\sigma} \frac{k'_\sigma}{2M_N} \right] \frac{(\not{p}_N + \not{k} + M_N)}{2p_N \cdot k} \left[ \gamma^\mu + \kappa_p i\sigma^{\mu\rho} \frac{k_\rho}{2M_N} \right] N(p_N, s_N), \quad (21)$$

$$\begin{aligned} \mathcal{M}_{c3}^{\nu\mu}(\gamma p \rightarrow \gamma \pi^0 p) &= -e^2 \frac{f_{\pi NN}}{m_\pi} \bar{N}(p'_N, s'_N) \left[ \gamma^\nu - \kappa_p i\sigma^{\nu\sigma} \frac{k'_\sigma}{2M_N} \right] \frac{(\not{p}'_N + \not{k}' + M_N)}{2p'_N \cdot k'} \\ &\times \not{p}_\pi \gamma_5 \frac{(\not{p}_N + \not{k} + M_N)}{2p_N \cdot k} \left[ \gamma^\mu + \kappa_p i\sigma^{\mu\rho} \frac{k_\rho}{2M_N} \right] N(p_N, s_N), \end{aligned} \quad (22)$$

$$\begin{aligned} \mathcal{M}_{c4}^{\nu\mu}(\gamma p \rightarrow \gamma \pi^0 p) &= -e^2 \frac{f_{\pi NN}}{m_\pi} \bar{N}(p'_N, s'_N) \left[ \gamma^\mu + \kappa_p i\sigma^{\mu\rho} \frac{k_\rho}{2M_N} \right] \frac{(\not{p}'_N - \not{k} + M_N)}{-2p'_N \cdot k} \\ &\times \not{p}_\pi \gamma_5 \frac{(\not{p}'_N - \not{k}' + M_N)}{-2p'_N \cdot k'} \left[ \gamma^\nu - \kappa_p i\sigma^{\nu\sigma} \frac{k'_\sigma}{2M_N} \right] N(p_N, s_N), \end{aligned} \quad (23)$$

$$\begin{aligned} \mathcal{M}_{c5}^{\nu\mu}(\gamma p \rightarrow \gamma \pi^0 p) &= -e^2 \frac{f_{\pi NN}}{m_\pi} \bar{N}(p'_N, s'_N) \left[ \gamma^\mu + \kappa_p i\sigma^{\mu\rho} \frac{k_\rho}{2M_N} \right] \frac{(\not{p}'_N - \not{k} + M_N)}{-2p'_N \cdot k} \\ &\times \left[ \gamma^\nu - \kappa_p i\sigma^{\nu\sigma} \frac{k'_\sigma}{2M_N} \right] \frac{(\not{p}'_N + \not{k}' - \not{k} + M_N)}{-2p'_N \cdot (k - k') - 2k \cdot k'} \not{p}_\pi \gamma_5 N(p_N, s_N), \end{aligned} \quad (24)$$

$$\begin{aligned} \mathcal{M}_{c6}^{\nu\mu}(\gamma p \rightarrow \gamma \pi^0 p) &= -e^2 \frac{f_{\pi NN}}{m_\pi} \bar{N}(p'_N, s'_N) \left[ \gamma^\nu - \kappa_p i\sigma^{\nu\sigma} \frac{k'_\sigma}{2M_N} \right] \frac{(\not{p}'_N + \not{k}' + M_N)}{2p'_N \cdot k'} \\ &\times \left[ \gamma^\mu + \kappa_p i\sigma^{\mu\rho} \frac{k_\rho}{2M_N} \right] \frac{(\not{p}'_N - \not{k} + \not{k}' + M_N)}{-2p'_N \cdot (k - k') - 2k \cdot k'} \not{p}_\pi \gamma_5 N(p_N, s_N). \end{aligned} \quad (25)$$

Note that all six amplitudes of Eqs.(20-25) are needed to satisfy gauge invariance with respect to both the incoming and outgoing photons.

#### IV. RESULTS FOR $\gamma P \rightarrow \gamma \pi^0 P$ OBSERVABLES AND DISCUSSION

Having described the model for the  $\gamma p \rightarrow \gamma \pi^0 p$  reaction, we now turn to the results. In order to have a point of comparison, we start by showing the result for the  $\gamma p \rightarrow \pi^0 p$  reaction corresponding to the mechanisms of Fig. 1. Our aim here is not to provide an accurate description of the  $\gamma p \rightarrow \pi^0 p$  reaction (which exists in the literature), but to see the intrinsic accuracy of the present effective Lagrangian formalism, which serves as our starting point for the corresponding mechanisms as shown in Fig. 2 for the  $\gamma p \rightarrow \gamma \pi^0 p$  reaction.

Fig. 3 shows the total cross section for the  $\gamma p \rightarrow \pi^0 p$  reaction. Although the  $\gamma p \rightarrow \pi^0 p$  cross section is clearly dominated by the  $\Delta$ -excitation mechanism, making it an informative tool to study the  $\Delta$ -resonance properties, additional non-resonant mechanisms are needed to obtain an accurate description. It is seen that at the lower energies, the main non-resonant contributions come from the nucleon Born diagrams. At the higher energies, the  $\Delta$ -excitation alone yields too large cross sections and is mainly reduced by the  $\omega$ -exchange mechanism, which dominates the high-energy behaviour of the  $\gamma p \rightarrow \pi^0 p$  reaction [24]. By comparing the total result in Fig. 3 with the accurate data, it is seen that the present effective Lagrangian model provides a rather good description below the  $\Delta$ -resonance position, underestimates the data around 325 MeV at the 10 % level, and has an accuracy at the 20 % level around 450 MeV. The systematic deviation of the present tree-level description with regard to the data as one moves through the  $\Delta$ -resonance, is well understood and originates

from  $\pi N$  rescattering (loop) contributions which restore unitarity. Although below two-pion production threshold, one can easily restore unitarity for the  $\gamma p \rightarrow \pi^0 p$  reaction by using the  $\pi N$  phase-shifts as phases of the pion photoproduction amplitude, the corresponding unitarization procedure for the  $\gamma p \rightarrow \gamma\pi^0 p$  reaction has not yet been worked out. In particular, for the  $\gamma p \rightarrow \gamma\pi^0 p$  reaction, care has to be taken to respect gauge invariance, as one can have intermediate  $\pi^+ n$  loop contributions where the photon couples to the intermediate charged pion. Such a gauge invariant unitary description of the  $\gamma p \rightarrow \gamma\pi^0 p$  reaction could be addressed within the context of a dynamical model, and seems to be a promising subject for future work. In the present paper, we explore as a first step the  $\gamma p \rightarrow \gamma\pi^0 p$  reaction within the context of the effective Lagrangian model of Fig. 2, in order to investigate promising kinematics and observables for the extraction of the  $\Delta^+$  magnetic dipole moment.

Passing next from the  $\gamma p \rightarrow \pi^0 p$  reaction to the description of the  $\gamma p \rightarrow \gamma\pi^0 p$  reaction, it is important to stress that the electric coupling of the emitted photon to the charged particles is completely constrained by gauge invariance as discussed in Sec. III. However the magnetic dipole moment of the  $\Delta^+$  (and also its smaller higher moments) is not fixed by general theoretical arguments and has to be extracted from a fit to experiment. Therefore, the only new parameter that appears in the present formalism for the  $\gamma p \rightarrow \gamma\pi^0 p$  reaction compared to the  $\gamma p \rightarrow \pi^0 p$  reaction, is the  $\Delta^+$  anomalous magnetic moment  $\kappa_{\Delta^+}$ . In the following, we investigate the sensitivity of different  $\gamma p \rightarrow \gamma\pi^0 p$  observables to this anomalous magnetic moment  $\kappa_{\Delta^+}$ .

Fig. 4 shows the dependence of the differential cross section of the  $\gamma p \rightarrow \gamma\pi^0 p$  reaction on the outgoing photon energy for three incoming photon energies through the  $\Delta$ -resonance region. The cross sections have been integrated over both photon and pion angles. The calculations compare the importance of the different mechanisms in Fig. 2, using the value  $\kappa_{\Delta^+} = 3$ . One clearly sees that the cross section for the resonant mechanism alone is dominated at the lower photon energies by the bremsstrahlung contributions (Fig. 2(a1) and (a3)), which show the typical  $1/E'_\gamma$  energy dependence. It is also seen that the non-resonant mechanisms induce, due to interference, a distinct energy dependence as one moves through the  $\Delta$ -resonance similar to the case of the  $\gamma p \rightarrow \pi^0 p$  reaction. Note in particular the partial cancellation of bremsstrahlung with  $\Delta$  and nucleon intermediate states for the smaller values of  $E'_\gamma$ .

The cross section for the  $\gamma p \rightarrow \gamma\pi^0 p$  reaction has been measured for the first time by the A2/TAPS Collaboration at MAMI [10]. Our total results in Fig. 4 compare favorably with the preliminary data in both incoming and outgoing photon energy dependence.

Fig. 5 shows the sensitivity of the angle integrated cross sections to the value of the  $\Delta^+$  anomalous magnetic moment. The sensitivity of these cross sections to  $\kappa_{\Delta^+}$  increases with increasing outgoing photon energy, but remains relatively modest even at the higher energies, where the difference between the  $\kappa_{\Delta^+} = 0$  and  $\kappa_{\Delta^+} = 3$  values is at the 10 - 15 % level.

In Fig. 6, we show the corresponding photon c.m. angular dependence of the cross sections integrated over the outgoing photon energy (for the cut  $E'_\gamma{}^{c.m.} > 90$  MeV) and over the pion angles. The angular dependence displays a broad maximum around a c.m. angle of  $110^\circ$ . The calculations show that the sensitivity of these integrated unpolarized cross sections to  $\kappa_{\Delta^+}$  lies at the 10 - 20 % level over most of the angular range. At an incoming photon energy of 450 MeV, a larger effect is observed around the forward and backward angles.

However, we found that the sensitivity to the  $\Delta^+$  anomalous magnetic moment can be

substantially increased when using a linearly polarized photon beam. In this case, one can define the photon asymmetry  $\Sigma \equiv (d\sigma_{\perp} - d\sigma_{\parallel}) / (d\sigma_{\perp} + d\sigma_{\parallel})$ , where  $d\sigma_{\perp}$  ( $d\sigma_{\parallel}$ ) are the differential cross sections for incoming photon polarization perpendicular (parallel) to the reaction plane spanned by the incoming and outgoing photon c.m. momentum vectors. The outgoing photon energy dependence of the photon asymmetry is shown in Fig. 7 where the differential cross sections  $d\sigma_{\perp}$  and  $d\sigma_{\parallel}$  are integrated over all photon and pion angles, corresponding to the situation in Fig. 5. In comparison with the unpolarized cross section shown in Fig. 5, one now obtains a clearly larger sensitivity to  $\kappa_{\Delta}^{+}$ , in particular at the larger values of  $E_{\gamma}^{\prime c.m.}$ .

One can further increase the sensitivity of the  $\gamma p \rightarrow \gamma \pi^0 p$  reaction to the  $\Delta^{+}$  magnetic dipole moment by measuring differential cross sections. In particular, by choosing those angular ranges where the photon is emitted in the backward hemisphere with respect to both protons (in the c.m. system) as shown in Fig. 8, one suppresses the bremsstrahlung contributions and largely increases the sensitivity to  $\kappa_{\Delta^{+}}$ . This is shown in Fig. 9 for the fully differential cross section of Eq. (3), which is differential w.r.t. the photon c.m. energy, the photon c.m. polar angle and the pion polar and azimuthal angles (the latter two are defined in the  $\pi^0 p$  rest frame). The differential cross sections in Fig. 9, shown for  $E_{\gamma} = 450$  MeV, are now peaked around  $E_{\gamma}^{\prime c.m.} = 100$  MeV due to the resonant- $\Delta$  contribution of Fig. 2(a2), which contains  $\kappa_{\Delta^{+}}$ . On the other hand, in the angle integrated cross sections shown in Fig. 5, the contribution of Fig. 2(a2) merely manifests itself in the shoulder at higher values of the outgoing photon energy  $E_{\gamma}^{\prime c.m.}$ . Furthermore, one sees from Fig. 9 that the maximum of the cross section for  $\kappa_{\Delta^{+}} = 0$  is reduced by about 30 % for the value  $\kappa_{\Delta^{+}} = 3$  as compared to  $\kappa_{\Delta^{+}} = 0$ . The corresponding photon asymmetry  $\Sigma$  reaches large values and also displays a very pronounced energy dependence. The differences resulting from various values of  $\kappa_{\Delta^{+}}$  is in the range predicted by different theoretical models, and should be clearly resolved by measurements of  $\Sigma$  at the 5 % level.

Although a measurement of the fivefold differential cross section is very tough due to the small count rates, we found that one can largely keep the sensitivity to  $\kappa_{\Delta}$  by integrating over a larger region of phase space around the kinematical situations where the photon is emitted in the backward hemisphere with respect to both protons. This is illustrated in Fig. 10 where the differential cross section is shown integrated over the forward hemisphere for the outgoing photon angle (w.r.t. the incoming photon direction in the c.m. system) and where the pion is emitted over the azimuthal angular range  $-90^{\circ} < \Phi_{\pi}^{*} < 90^{\circ}$ . One sees from Fig. 10 that the cross section at 450 MeV shows a 20 % sensitivity, and at 500 MeV a 30 % sensitivity, to the difference between  $\kappa_{\Delta^{+}} = 0$  and  $\kappa_{\Delta^{+}} = 3$ . Furthermore, by comparing for a value  $\kappa_{\Delta^{+}} = 3$ , the full result with the  $\Delta$  anomalous magnetic moment contribution separately (diagram Fig. 2 (a2)), one sees that the latter yields the dominant contribution to the total result at the higher outgoing photon energies for 450 MeV and 500 MeV initial photon energies. By comparing the partially integrated cross section of Fig. 10 at 450 MeV to the cross section of Fig. 5, one sees that it reaches about one fifth of the cross section integrated over the full angular range. As the cross section of Fig. 5 has already been measured [10], the cross sections of Fig. 10 could be accessible through a dedicated experiment. In view of the characteristic angular dependence of the effect under investigation, a full  $4\pi$  coverage will be a prerogative to obtain more significant information on the magnetic dipole moment of the  $\Delta$ . Such a  $4\pi$  detector will allow one to increase the count rate substantially w.r.t. the present TAPS experiment, and thus to select kinematical

ranges where background (bremsstrahlung) effects are strongly suppressed as is shown in Fig. 10.

Finally, we show in Fig. 11 the photon asymmetries corresponding to the partially integrated cross sections of Fig. 10. Compared to the asymmetries of Fig. 7, where the cross sections were integrated over all photon and pion angles, both the magnitude of the asymmetries in Fig. 11 and the sensitivity to  $\kappa_{\Delta}$  are larger. Therefore, a dedicated experiment consisting of a  $4\pi$  detector and a high intensity polarized photon beam, promises to provide a good opportunity to extract the  $\Delta^+$  magnetic dipole moment from the  $\gamma p \rightarrow \gamma\pi^0 p$  reaction. Such an experiment is planned using the Crystal Ball detector in combination with the polarized photon beam at MAMI [11].

## V. CONCLUSIONS

In this paper we investigated the  $\gamma p \rightarrow \gamma\pi^0 p$  process as a tool to access the  $\Delta^+(1232)$  magnetic dipole moment.

An effective Lagrangian formalism to describe the  $\gamma p \rightarrow \pi^0 p$  reaction in the  $\Delta(1232)$  resonance region, served as a starting point to develop a corresponding model of the  $\gamma p \rightarrow \gamma\pi^0 p$  reaction. When extending the model of the  $\gamma p \rightarrow \pi^0 p$  process to the  $\gamma p \rightarrow \gamma\pi^0 p$  process, the electric coupling of the additional photon to the charged particles is completely constrained by gauge invariance. In particular, we paid special attention to the constraint that gauge invariance imposes on the coupling of a photon to a resonance of finite width. In analogy to the case of the  $W^\pm$  vector boson, which has been discussed extensively in recent years in the literature, we follow a complex mass scheme procedure where the amplitude for the  $\gamma p \rightarrow \gamma\pi^0 p$  process which involves the  $\Delta^+(1232)$  resonance, is Laurent expanded around the complex pole position of the resonance. This procedure guarantees electromagnetic gauge invariance. In comparison with the  $\gamma p \rightarrow \pi^0 p$  reaction, the only new parameter which enters in the description of the  $\gamma p \rightarrow \gamma\pi^0 p$  reaction in the  $\Delta(1232)$  region is the  $\Delta^+$  anomalous magnetic moment  $\kappa_{\Delta^+}$ . We then investigated the sensitivity of various  $\gamma p \rightarrow \gamma\pi^0 p$  observables to this anomalous magnetic moment  $\kappa_{\Delta^+}$ .

We first compared the unpolarized  $\gamma p \rightarrow \gamma\pi^0 p$  cross section integrated over the whole photon and pion angular range. For this fully angle integrated cross section, the resonant mechanism is dominated by the bremsstrahlung contribution which shows the typical  $1/E'_\gamma$  dependence in the outgoing photon energy  $E'_\gamma$ . We also found that the non-resonant mechanisms induce, due to interference, a distinct energy pattern as one moves through the  $\Delta$ -resonance. Our calculations compare favorably with preliminary data for those fully integrated cross sections.

The sensitivity of the unpolarized  $\gamma p \rightarrow \gamma\pi^0 p$  cross section integrated over the whole photon and pion angular range to  $\kappa_{\Delta^+}$ , was found to increase with increasing photon energy, but remains relatively modest. At an incoming photon energy of 450 MeV, the difference between the  $\kappa_{\Delta^+} = 0$  and  $\kappa_{\Delta^+} = 3$  values is at the 10 - 15 % level.

However, one can further increase the sensitivity to  $\kappa_{\Delta^+}$  by measuring differential cross sections. In particular, by selecting the kinematical situations where the photon is emitted in the backward hemisphere w.r.t. both protons, the bremsstrahlung contribution to the cross sections is largely suppressed. When partially integrating the cross sections around these backward angle kinematics, we found that, for an incoming photon energy range of

450 - 500 MeV, the difference between the  $\kappa_{\Delta^+} = 0$  and  $\kappa_{\Delta^+} = 3$  values is at the 20 - 30 % level.

Furthermore, we showed that the sensitivity to the  $\Delta$  anomalous magnetic moment can be even more increased by using a linearly polarized photon beam. At the higher outgoing photon energies, the asymmetries are at the 10 - 30 % level through the  $\Delta$  region and display a clear sensitivity to  $\kappa_{\Delta^+}$ .

In view of our findings, a dedicated experiment using a  $4\pi$  detector and a high intensity photon beam seems to be a promising experiment to extract the  $\Delta^+$  magnetic dipole moment from the  $\gamma p \rightarrow \gamma\pi^0 p$  reaction. The model developed in this paper can serve as a first step for such an extraction. The measurement of the  $\Delta$  magnetic dipole moment will provide us with new information on baryon structure which can be confronted with various baryon structure calculations.

### ACKNOWLEDGMENTS

It is a pleasure to acknowledge fruitful conversations with R. Beck, M. Kotulla, V. Metag, B. Nefkens, G. Rosner, and L. Tiator. This work was supported by the Deutsche Forschungsgemeinschaft (SFB 443).

## REFERENCES

- [1] T.M. Aliev, A. Özpineci, and M. Savci, Phys. Rev. D **62**, 053012 (2000).
- [2] T.M. Aliev, A. Özpineci, and M. Savci, Nucl. Phys. **A678**, 443 (2000).
- [3] L.A. Kondratyuk und L.A. Ponomarov, Yad. Fiz. **7**, 11 (1968) [Sov. J. Nucl. Phys. **7**, 82 (1968)].
- [4] B.M.K. Nefkens *et al.*, Phys. Rev. D **18**, 3911 (1978).
- [5] A. Bosshard *et al.*, Phys. Rev. D **44**, 1962 (1991).
- [6] D.E. Groom *et al.* (PDG), Eur. Phys. J. **C15**, 1 (2000).
- [7] M.M. Giannini, in *Proceedings of the Workshop Perspectives on Nuclear Physics at Intermediate Energies, ICTP Trieste, Italy, 1983 (World Scientific, Singapore, 1984)*; and D. Drechsel, in MAMI funding proposal to DFG, SFB 201 (1984-86), p. 56.
- [8] A.I. Machavariani, A. Faessler, and A. J. Buchmann, Nucl. Phys. **A646**, 231 (1999); Nucl. Phys. **A686**, 601 (E) (2001).
- [9] D. Drechsel, M. Vanderhaeghen, M.M. Giannini, and E. Santopinto, Phys. Lett. B **484**, 236 (2000).
- [10] M. Kotulla (for the A2/TAPS collaboration), in *Proceedings of the Workshop on The Physics of Excited Nucleons (Nstar 2001), Mainz, Germany, 2001, (World Schientific, Singapore, to be published)*.
- [11] R. Beck, B. Nefkens *et al.*, Letter of Intent, MAMI (2001).
- [12] M. El Amiri, G. López Castro, and J. Pestieau, Nucl. Phys. **A543**, 673 (1992).
- [13] G. López Castro and A. Mariano, nucl-th/0010045.
- [14] L.M. Nath, B. Etemadi, and J.D. Kimel, Phys. Rev. D **3**, 2153 (1971).
- [15] D. Drechsel, O. Hanstein, S. Kamalov, and L. Tiator, Nucl. Phys. **A645**, 145 (1999).
- [16] R. Beck, H.P. Krahn *et al.*, Phys. Rev. C **61**, 035204 (2000).
- [17] A. Sirlin, Phys. Rev. Lett. **67**, 2127 (1991); Phys. Rev. Lett. **86**, 389 (2001).
- [18] R.G. Stuart, Phys. Rev. Lett. **70**, 3193 (1993).
- [19] H. Veltman, Z. Phys. C **62**, 35 (1994).
- [20] G. López Castro, J.L. Lucio M., and J. Pestieau, Int. J. Mod. Phys. A **11**, 563 (1996); hep-ph/9504351.
- [21] U. Baur and D. Zeppenfeld, Phys. Rev. Lett. **75**, 1002 (1995).
- [22] M. Beuthe, R. Gonzalez Felipe, G. López Castro, and J. Pestieau, Nucl. Phys. **B498**, 55 (1997).
- [23] G. López Castro and G. Toledo Sánchez, Phys. Rev. D **61**, 033007 (2000).
- [24] M. Guidal, J.M. Laget, and M. Vanderhaeghen, Nucl. Phys. **A627**, 645 (1997).
- [25] M.M. Pavan, R.A. Arndt, I.I. Strakovsky, and R.L. Workman,  $\pi$ N Newslett. **15**, 171 (1999).
- [26] M. MacCormick *et al.*, Phys. Rev. C **53**, 41 (1996).
- [27] J. Ahrens *et al.*, Phys. Rev. Lett. **84**, 5950 (2000).

FIGURES

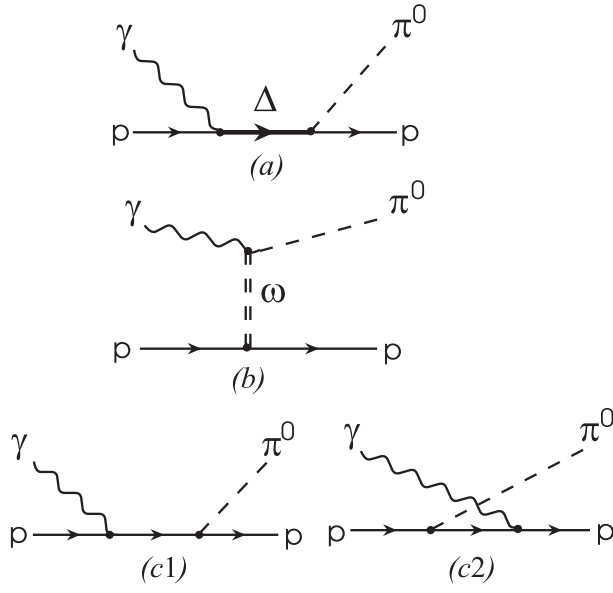


FIG. 1. Diagrams for the  $\gamma p \rightarrow \pi^0 p$  reaction in the  $\Delta(1232)$  region, serving as starting point for the calculation of the  $\gamma p \rightarrow \gamma \pi^0 p$  reaction :  $\Delta$ -resonance excitation (a),  $\omega$ -exchange (b), and Born diagrams (c1,c2).

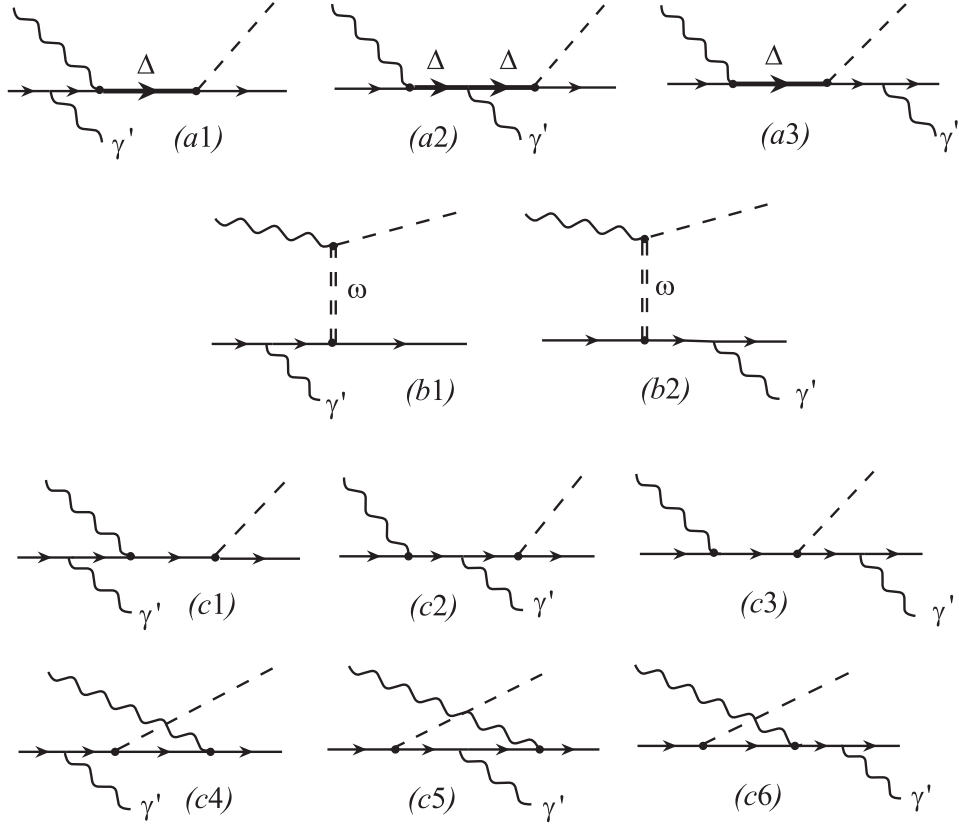


FIG. 2. Diagrams considered in the calculation of the  $\gamma p \rightarrow \gamma' \pi^0 p$  reaction in the  $\Delta(1232)$  region, obtained by gauge invariant coupling of a photon to the diagrams of Fig. 1. This yields the  $\Delta$ -resonance diagrams (a1-a3),  $\omega$ -exchange diagrams (b1-b2), and Born diagrams where the photon is emitted from all proton lines (c1-c6). Note that, with respect to the outgoing photon, the sum of the three diagrams (a1-a3) is gauge invariant, and the sum of (b1-b2) is gauge invariant. Furthermore, for the Born terms, the six diagrams (c1-c6) are required to satisfy gauge invariance with respect to both the incoming and outgoing photons. In comparison with the diagrams of Fig. 1 for  $\gamma p \rightarrow \pi^0 p$ , there is only *one* new parameter which enters here at the  $\gamma\Delta\Delta$  vertex (a2), namely the  $\Delta^+$  anomalous magnetic moment  $\kappa_{\Delta^+}$ .



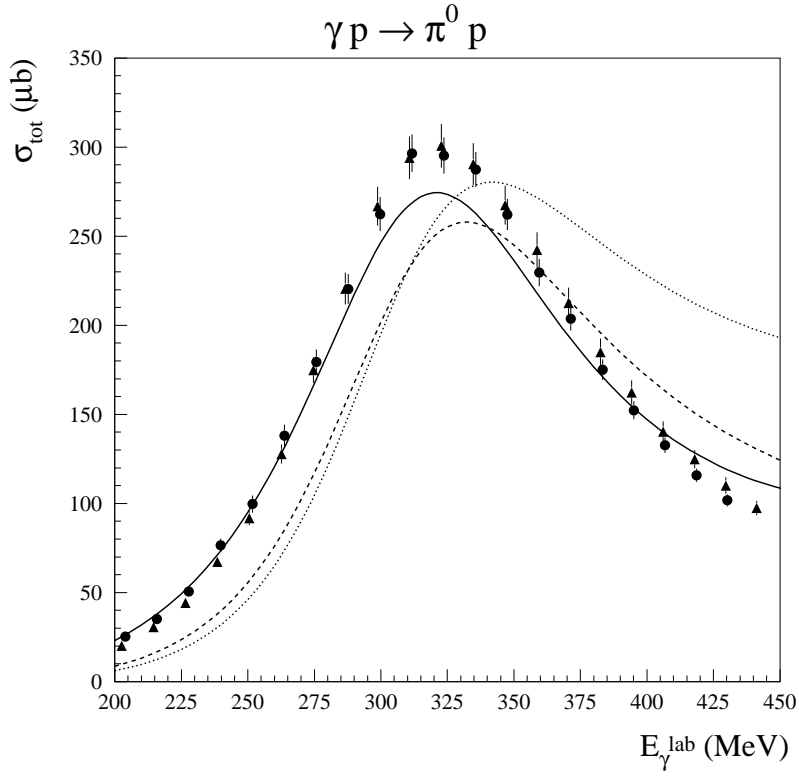


FIG. 3. Total cross section for the  $\gamma p \rightarrow \pi^0 p$  reaction in the  $\Delta(1232)$ -region. The calculations correspond to the mechanisms of Fig. 1 :  $\Delta$ -excitation (dotted curve),  $\Delta + \omega$ -exchange (dashed curve), and the sum of the three mechanisms (full curves). The difference between the full curves and the data is understood as originating mainly from  $\pi N$  rescattering mechanisms. The MAMI data are from Ref. [26] (circles) and from Ref. [27] (triangles).

$$\gamma p \rightarrow \gamma \pi^0 p : \kappa_{\Delta^+} = 3$$

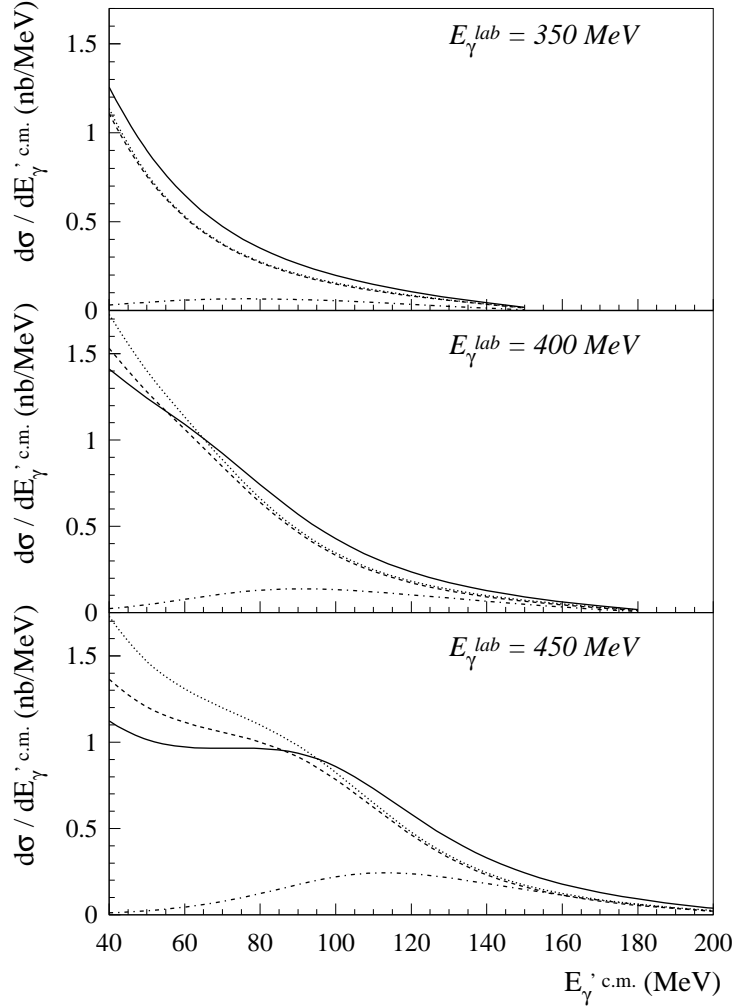


FIG. 4. Outgoing photon c.m. energy dependence of the cross section  $d\sigma/dE_\gamma^{c.m.}$  (integrated over photon and pion angles) of the  $\gamma p \rightarrow \gamma \pi^0 p$  reaction. The calculation with only the  $\Delta$  anomalous magnetic moment contribution (a2) of Fig. 2 is shown by the dashed-dotted curves. The calculation of the  $\Delta$ -resonance mechanisms (a1-a3) of Fig. 2 is shown by the dotted curves. The sum of  $\Delta$ -resonance and  $\omega$ -exchange mechanisms (diagrams (b1-b2) of Fig. 2) is given by the dashed curves, and the sum of all mechanism of Fig. 2 (including the Born terms (c1-c6)) is given by the full curves. The value of the  $\Delta^+$  anomalous magnetic moment was set equal to  $\kappa_{\Delta^+} = 3$ .

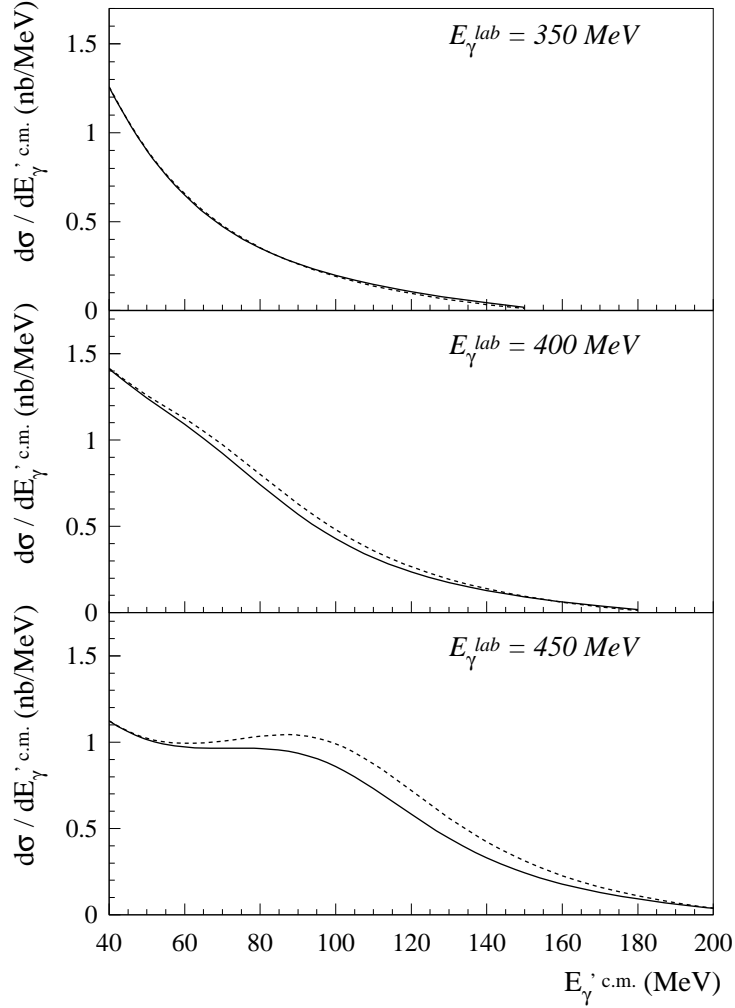
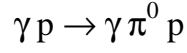


FIG. 5. Outgoing photon c.m. energy dependence of the cross section  $d\sigma/dE_\gamma^{c.m.}$  (integrated over photon and pion angles) of the  $\gamma p \rightarrow \gamma \pi^0 p$  reaction. The calculations are the total results (including all diagrams of Fig. 2) for the values :  $\kappa_{\Delta^+} = 0$  (dashed curves) and  $\kappa_{\Delta^+} = 3$  (full curves).

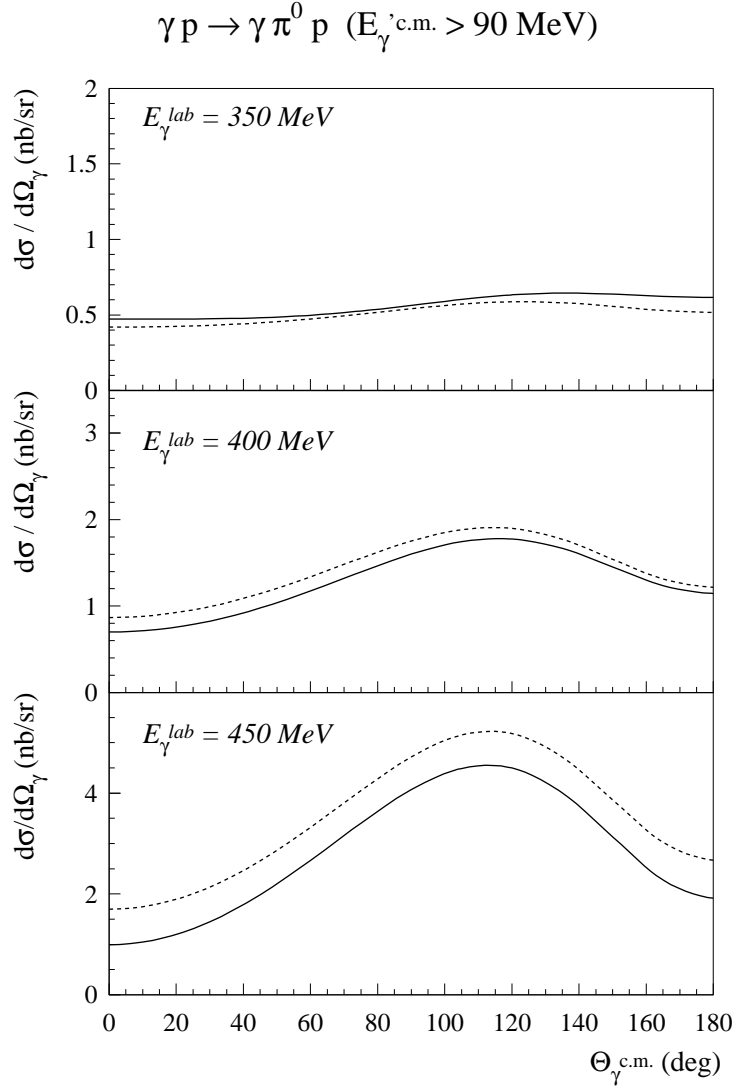


FIG. 6. Outgoing photon c.m. angular dependence of the cross section  $d\sigma/d\Omega_\gamma^{\text{c.m.}}$  of the  $\gamma p \rightarrow \gamma \pi^0 p$  reaction. The cross section is integrated over the pion angles and over the outgoing photon energy range  $E_\gamma^{\text{c.m.}} > 90$  MeV. The calculations are the total results (including all diagrams of Fig. 2) for the values :  $\kappa_{\Delta^+} = 0$  (dashed curves) and  $\kappa_{\Delta^+} = 3$  (full curves).

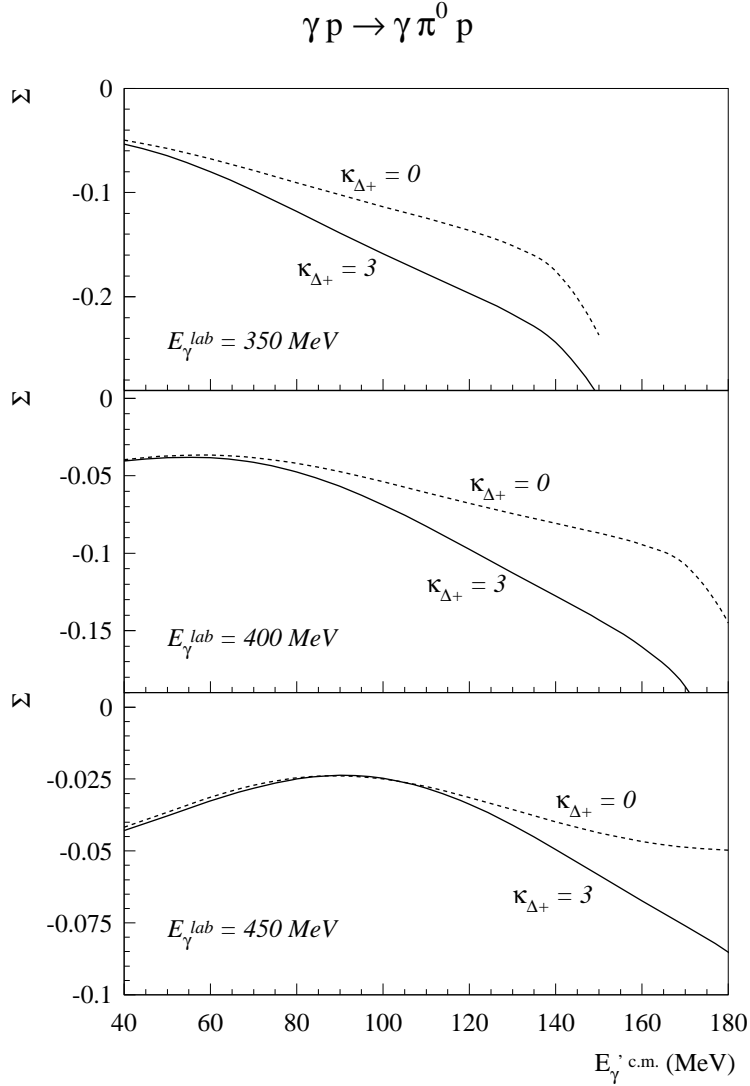


FIG. 7. Outgoing photon c.m. energy dependence of the  $\gamma p \rightarrow \gamma \pi^0 p$  photon asymmetry  $\Sigma$ , integrated over the photon and pion angles, and differential w.r.t. the outgoing photon energy  $E'_\gamma$ , as in Fig. 5. The calculations are the total results (including all diagrams of Fig. 2), for the two values of  $\kappa_{\Delta^+}$  as indicated on the curves.

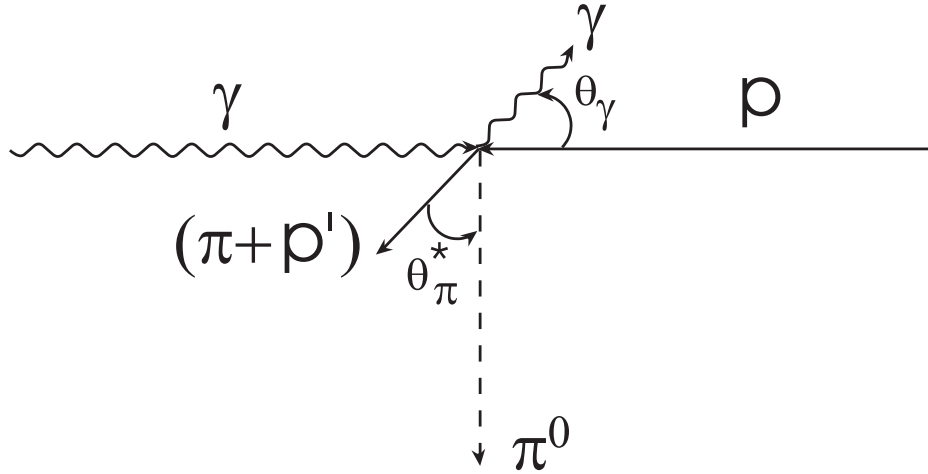


FIG. 8. Definition of angles of the  $\gamma p \rightarrow \gamma \pi^0 p$  reaction :  $\theta_\gamma$  is the photon angle in the c.m. system,  $\theta_\pi^*$  is the pion angle in the  $(\pi^0 p)$  rest frame w.r.t. the direction of the  $(\pi^0 p)$  c.m. momentum. The pion momentum displayed in the figure corresponds to an out-of-plane angle  $\Phi_\pi^* = 0^\circ$ .

$\gamma p \rightarrow \gamma \pi^0 p : E_{\gamma}^{\text{lab}} = 450 \text{ MeV}$

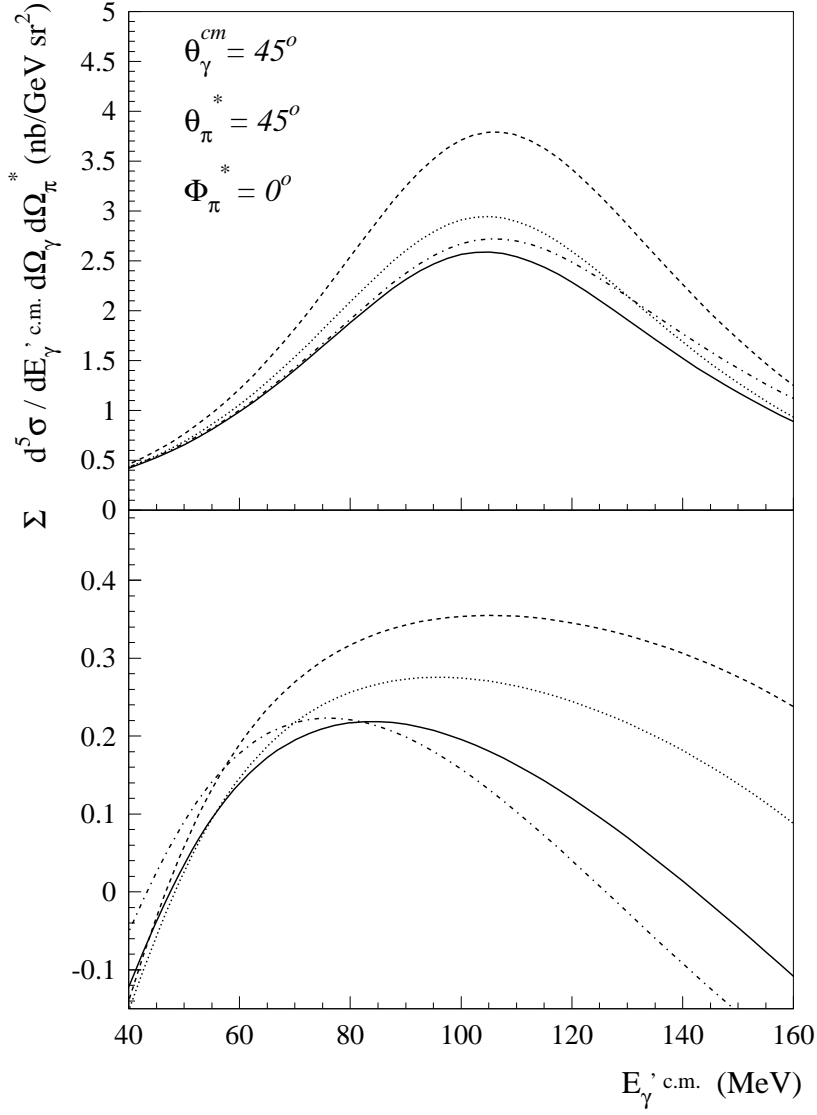


FIG. 9. Five-fold differential cross section  $d^5\sigma$  (upper panel), and corresponding photon asymmetry  $\Sigma$  (lower panel) for the  $\gamma p \rightarrow \gamma \pi^0 p$  reaction as function of the outgoing photon c.m. energy. The angles are defined as in Fig. 8, and the kinematics considered here corresponds (approximately) to the situation depicted in that figure. The calculations are the total results (including all diagrams of Fig. 2), for the values :  $\kappa_{\Delta^+} = 0$  (dashed curves),  $\kappa_{\Delta^+} = 1.5$  (dotted curves),  $\kappa_{\Delta^+} = 3$  (full curves),  $\kappa_{\Delta^+} = 4.5$  (dashed-dotted curves).

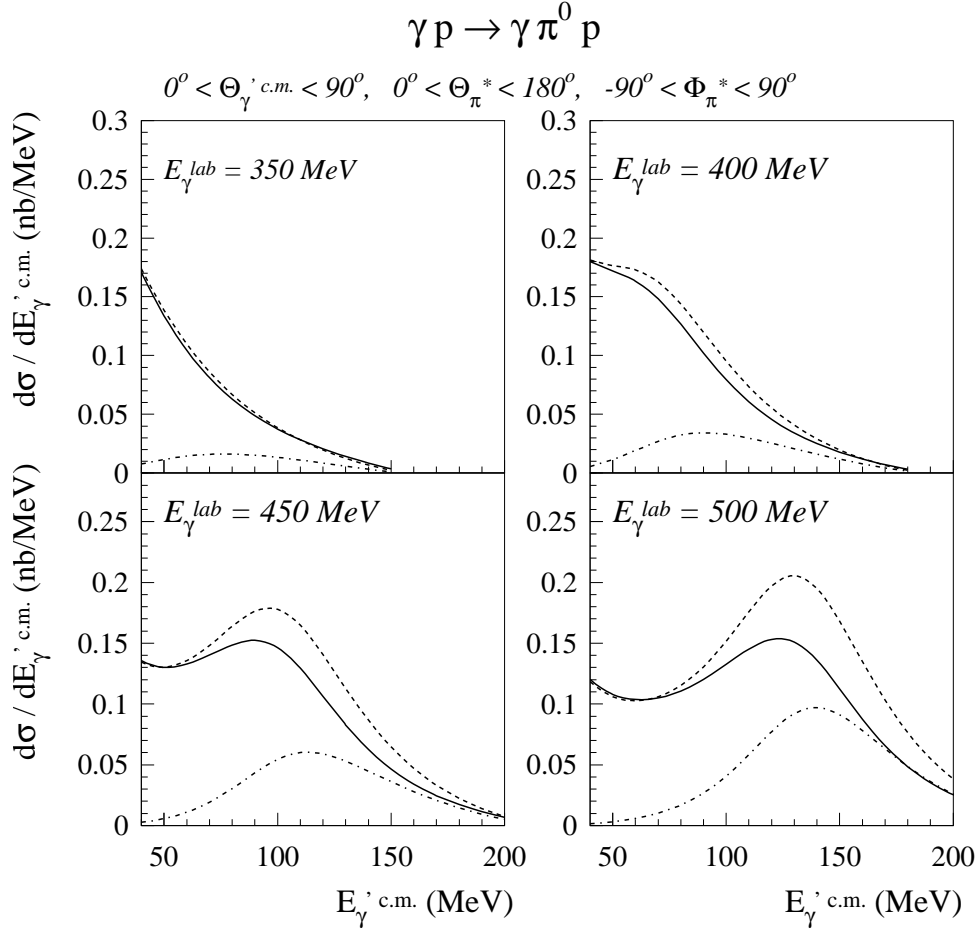


FIG. 10. Outgoing photon c.m. energy dependence of the  $\gamma p \rightarrow \gamma \pi^0 p$  cross section  $d\sigma/dE_\gamma^{c.m.}$ , partially integrated over the photon and pion angles as indicated. The calculations are the total results (including all diagrams of Fig. 2) for the values :  $\kappa_{\Delta^+} = 0$  (dashed curves) and  $\kappa_{\Delta^+} = 3$  (full curves). For comparison, the calculation with only the  $\Delta$  anomalous magnetic moment contribution (a2) of Fig. 2 for the value  $\kappa_{\Delta^+} = 3$  is shown by the dashed-dotted curves.



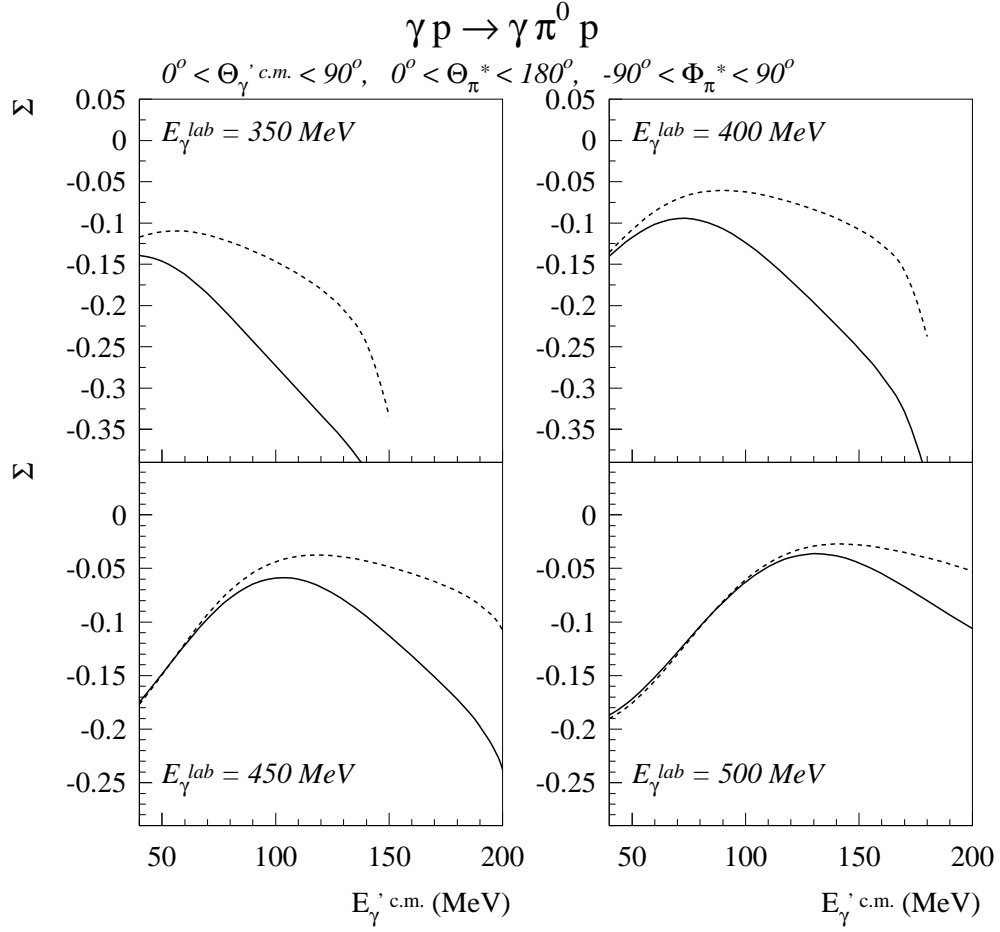


FIG. 11. Outgoing photon c.m. energy dependence of the  $\gamma p \rightarrow \gamma \pi^0 p$  photon asymmetry  $\Sigma$ , partially integrated over the photon and pion angles as indicated, and differential w.r.t. the outgoing photon energy  $E_\gamma^{c.m.}$ , as in Fig. 10. The calculations are the total results (including all diagrams of Fig. 2), for the values :  $\kappa_{\Delta^+} = 0$  (dashed curves) and  $\kappa_{\Delta^+} = 3$  (full curves).